Z. angew. Math. Phys. 49 (1998) 849–868
0044-2275/98/060849-20 $ 1.50+0.20/0

Zeitschrift für angewandte Mathematik und Physik ZAMP

A hybrid multiple scale procedure for boundary layers involving several dissimilar scales

Joseph Majdalani

Abstract. For a class of boundary-value problems involving damped oscillations that occur at three or more dissimilar scales, both matched asymptotic and multiple scale expansions can fail to provide uniformly valid solutions. A novel approach is introduced in this paper that suggests determining a composite scale that matches the dissimilar scales, in lieu of the asymptotic solutions, in their applicable domains. Information contained in the dissimilar scales is condensed into one composite scale, thus reducing the number of independent scales to two. For that purpose, a procedure is presented herein that consists of: 1) identifying the form and location of prevalent characteristic scales, 2) determining a composite scale that matches the stretched or contracted scales in their respective intervals, and 3) invoking a two-variable multiple scale method that employs the composite scale as one of its independent variables. This procedure is applied successfully to a problem that eludes conventional perturbation methods. The corresponding boundary-layer equation pertains to the separable transversely-dependent component of the rotational momentum equation used in modeling oscillatory flows in low aspect ratio rectangular channels where blowing is present at the walls. An expansion series is constructed in the parameter associated with small viscosity. A uniformly valid expression is extracted that captures the physical effects of unsteady inertia, viscous diffusion, and transverse convection of unsteady vorticity, while clearly showing that spatial attenuation of rotational waves is controlled by a single similarity parameter. Analytical results are numerically verified for a wide range of physical parameters and test cases.

Mathematics Subject Classification (1991). 76N20, 34E10, 76D30, 35D99, 34E99.

Keywords. Boundary-layer theory, perturbations, multiple scales, asymptotic expansions, oscillations.

1. Introduction

It is well-known (see for instance [3], [6], or [8]) that many boundary-value problems involving rapidly decaying oscillations can be put into the form

$$\varepsilon\frac{d^2f}{dx^2}+a(x)\frac{df}{dx}+b(x)f=0;\quad x\in[0,1] \tag{1.1}$$

where $0<\varepsilon\ll 1$, $a(x)$ and $b(x)$ are continuous functions of x, and where f varies rapidly in some regions of x. When several characteristic scales arise in the

problem, approximate solutions to (1.1) are typically constructed using matched asymptotic expansions or the methods of multiple scales. When f does not vary on a single scale in specific regions of the domain of interest but rather varies with widely dissimilar scales in isolated regions of the domain, matched asymptotic expansions are rendered useless (see Wilcox [8]). In such cases, even the methods of multiple scales are not guaranteed to succeed due to intractable obstructions, especially in problems involving three or more disparate scales (see Murdock [6] and [7]).

The aim of this paper is to devise a method to solve a problem that has eluded known perturbation methods, involving four widely varying scales for the independent variable. The dissimilar scales arise due to the presence of damping on top of rapid spatial attenuation in a boundary layer of the oscillatory type. The result is a problem that incorporates the characters of conventional boundary layers and damped oscillators. Having exhausted other available means, a two-variable multiple scale expansion is found by the author to be the only promising technique for extracting a uniformly valid solution for the case at hand. Since a multiple scale technique that employs three or four scales is unproductive in this problem, the technique had to be restricted to two variables, with the first one being the unmodified independent variable itself, as implicitly required by multiple scale formalism [8]. When the second variable is taken to be any one of the remaining scales, the resulting two-variable solution is found to be valid only in the interval where the corresponding modified scale is applicable. Inasmuch as matching the particular two-variable solutions is not feasible, and in recognition of the difficulties inherent in establishing a suitable, uniformly valid solution, an effective alternative is proposed that consists of devising a composite scale that matches the modified scales in their corresponding domains before invoking a two-variable multiple scale procedure. Employing such a composite scale, which is reducible to the dissimilar scales in their corresponding intervals, will lead to an accurate, uniformly valid solution.

The "hybrid" approach to be employed borrows the idea of matching solutions over intervals of validity from matched asymptotic expansions and applies it to the scales instead of the solutions, in order to reduce a multi-variable to a two-variable multiple scale problem. To that end, we offer the following systematic plan: In section 2, the governing differential equation is specified along with its boundary conditions. In section 3, a successful methodology is implemented to identify the independent scales. In section 4, a composite scale that matches the independent scales in their corresponding domains is constructed. In section 5, a generalized two-variable multiple scale expansion is derived leading to i) a uniformly valid solution, when the second variable is taken to be the composite scale, and ii) particular solutions that are valid in limited domains, when the second variable is taken to be the corresponding characteristic scale. Discussion of results is deferred to section 6 where analytical predictions are shown to compare quite favorably with corresponding numerical data. The leading-order term of the composite-

scale solution is shown therein to be in accord with the corresponding numerical solution in a wide range of physical parameters, in addition to capturing the key physical elements in the problem, and furnishing, as a bonus, a new similarity parameter that controls the solution's depth of penetration. Last, in section 7, a well-known technique is used to ascertain the order of accuracy associated with the composite-scale expansions.

Despite the wealth of singular perturbation methods for ordinary differential equations cited in the literature, a similar scale-matching procedure that is used in conjunction with multiple scales does not seem to have been addressed previously. The reader is referred, for instance, to the works of Kevorkian and Cole [3], Murdock [6], and Wilcox [8], and the references therein, spanning over a century of work in the field.

Far from being limited to a particular application, the method to be furnished herein offers new possibilities to solve boundary-layer problems involving several scales by first reducing the number of scales before invoking two-variable multiple scale expansions. The author's experience with the procedure has indicated its effectiveness in several problems of practical interest.

2. Problem formulation

In recent years much attention has been given to small amplitude steady-periodic pressure waves through fluids confined in rigid tubes. Though a problem of long intrinsic interest to acousticians and fluidicians, research has recently been spurred on by technological developments and the desire for better mathematical models of combustion processes and biological flows. Such models become more challenging when the tube walls are made permeable in a manner to allow steady injection or suction of a fluid. Naturally, the coupling between steady and small amplitude oscillatory velocities leads to a more complicated mathematical model that, heretofore, has been a deterrent to fruitful endeavors.

The problem that we propose to investigate arises in such an environment where an oscillatory field is established in a long rectangular channel of height $2h$ and width w, where $2h/w \ll 1$. Reminiscent of a flow between two infinitely long, parallel and permeable plates, two-dimensionality can be assumed in addition to symmetry with respect to the midsection plane that is equidistant from the walls. Gravity and lateral edge effects in the rectangular channel are ignored. The difference here from previous models is that steady injection is imposed at the porous walls, with a blowing speed of V_b. The radian frequency of oscillations corresponding to the fundamental or one of the overtones of the oscillating source is ω, the kinematic viscosity is ν, and c is the mean speed of sound. Due to symmetry, the analysis is limited to the domain extending from the wall to the plane of symmetry which, in two dimensions, will be referred to herein as the centerline.

Having briefly described the physical boundaries, we proceed to consider the governing equation arising in the model, similar in form to (1.1), and which corresponds to the separable transverse component of the rotational momentum equation (given in [4]):

$$\varepsilon\frac{d^2V_n}{dy^2}-\sigma\cos\left(\frac{\pi}{2}y\right)\frac{dV_n}{dy}+\left[i-\frac{\pi}{2}\sigma(1+\lambda_n)\sin\left(\frac{\pi}{2}y\right)\right]V_n=0;\quad y\in[0,1] \tag{2.1}$$

where y is the distance from the wall, normalized by h, and $V_n(y)$ is the component of the rotational velocity, normalized by the irrotational acoustic amplitude, which must satisfy two auxiliary conditions:

$$V_n(0)=1 \text{ (no-slip at the wall)} \tag{2.2}$$

$$V_n'(1)=0 \text{ (centerline symmetry)} \tag{2.3}$$

Equation (2.1) is known to the order of the injection Mach number, $M_b=V_b/c=O(10^{-3})$. The small parameters ε and σ are reciprocals of the dynamic similarity parameters Re_k and St, representing the kinetic Reynolds number and Strouhal number, respectively:

$$\varepsilon=Re_k^{-1}=v\omega^{-1}h^{-2} \tag{2.4}$$

$$\sigma=St^{-1}=V_b\omega^{-1}h^{-1} \tag{2.5}$$

We exploit the fact that Re_k is large, being the quadratic ratio of the domain height h, and the Stokes layer $\sqrt{v/\omega}$, which is an exceedingly small quantity. The real constant that appears in (2.1), $\lambda_n=2n+1$, $n=0,1,2,\ldots$, is an odd integer, and $i=\sqrt{-1}$. For physically meaningful settings, one should consider $St>10$ and $Re_k>10^5$, corresponding to $\varepsilon\ll\sigma\ll1$.

From a physical standpoint, the first term in (2.1) represents viscous diffusion, the second represents convection, and the third is the result of time-dependent inertia and coupling with mean flow components. The variable coefficient multiplying the convective term is found to be negative everywhere except at $y=1$, where it vanishes. Since it is not strictly negative everywhere, perturbation theory no longer guarantees a boundary layer near $y=1$ [8].

3. Characteristic scale identification

As indicated earlier, the first methodical step is to determine the form and location of the scales. The basic idea that we will employ is that the scales represent the order according to which the solution varies locally. Effectively, every characteristic scale that we seek to identify must correspond to the coordinate transformation that is capable of providing a balance in (2.1) between terms that are locally significant in specific intervals of the solution domain.

3.1. Contraction near the wall

Near the wall, the effect of sidewall injection is appreciable. The thin viscous layer that is typically established near the wall in steady flows is "blown off" the solid boundary in this problem to a nonlocalized region. A viscous layer of similar character was first identified in steady flows incorporating sidewall injection by Cole and Aroesty [2]. As a consequence of strong blowing at the wall, unsteady inertia and mean flow convection dominate. By contrast to the inner region in steady boundary layers where scale magnification of the form $y_1 = y/\varepsilon$ is necessitated, unconventional scaling is required here to achieve a balance between convection and inertia. Note that the solution to the problem obtained by keeping the two terms in (2.1) that dominate near the wall results in a wave of constant amplitude (to read: that varies extremely slowly). Since stretching is needed when amplitudes vary rapidly, contraction is needed here. Introducing the near-wall transformation variable, $y_1 = \varepsilon y$, (2.1) becomes:

$$\varepsilon^3 \frac{d^2 V_n}{dy_1^2} - \varepsilon \sigma U_y \frac{dV_n}{dy_1} + \left[i - \frac{\pi}{2} \sigma (1 + \lambda_n) \sin\theta \right] V_n = 0 \tag{3.1}$$

where $\theta = \pi y/2$ is a recurring action coordinate, and $U_y = \cos\theta$ is a function denoting the steady transverse velocity. A balance between inertia and convection is achieved in (2.1) since the actual velocity gradient near the wall is expected, and can be shown *a posteriori*, to be large; in other words,

$$\varepsilon \sigma U_y \frac{dV_n}{dy_1} = \sigma U_y \frac{dV_n}{dy} = O(1) \text{ since } \frac{dV_n}{dy} = O(\sigma^{-1}) = O(St) \tag{3.2}$$

3.2. Stretching near the centerline

At $y = 1$, the convective term becomes insignificant as U_y vanishes. A stretching of the scale is required here since the spatial wavelength, which is controlled by U_y, vanishes as well. Introducing the nontraditional scale, $y_1 = \varepsilon(1 - y)^{-q}$, a balance between unsteady inertia and diffusion can be achieved in (2.1):

$$q^2 \varepsilon^{1-2/q} \left[y_1^{2(1+1/q)} \frac{d^2 V_n}{dy_1^2} + \left(1 + \frac{1}{q} \right) y_1^{(1+2/q)} \frac{dV_n}{dy_1} \right] + \left[i - \frac{\pi}{2} \sigma (1 + \lambda_n) \sin\theta \right] V_n \tag{3.3}$$
$$= q \sigma \varepsilon^{-1/q} y_1^{(1+1/q)} U_y \frac{dV_n}{dy_1} \to 0$$

where the first two terms representing viscous and inertial forces will be of the same order when $\varepsilon^{1-2/q} = 1$, or $q = 2$.

Careful scaling shows that, in the vicinity of the previous location, viscous and convective terms must be in balance as well. When U_y is no longer negligible, a

value of $q = 1$ will characterize this scale at $y = y_u$, where y_u is undetermined. A balance between convection and viscous diffusion is achieved between the first two terms in (2.1) when $\varepsilon^{1-2/q} = \varepsilon^{-1/q}$, or $q = 1$:

$$q^2\varepsilon^{1-2/q}\left[y_1^{2(1+1/q)}\frac{d^2V_n}{dy_1^2} + \left(1+\frac{1}{q}\right)y_1^{(1+2/q)}\frac{dV_n}{dy_1}\right] - q\sigma\varepsilon^{-1/q}y_1^{(1+1/q)}U_y\frac{dV_n}{dy_1}$$
$$= -\left[i - \frac{\pi}{2}\sigma(1+\lambda_n)\sin\theta\right]V_n \tag{3.4}$$

The stretching exponent thus varies between $q = 1$ (where convection and diffusion are in balance at $y = y_u$) and $q = 2$ (where diffusion and inertia are in balance at $y = 1$) in the small interval of undetermined size corresponding to $y_u < y < 1$. Clearly, all three mechanisms must be present as y varies between y_u and 1. Using the limiting scales to provide us with an alternative of replacing the local physical process by its "average," the scaling exponent characterizing the thin near-centerline region is taken to be $q = 3/2$, resulting in a balance of all three forces. In this fashion, it can be argued that $y_1 = \varepsilon(1-y)^{-3/2}$ can be used, when compelled by the need to reduce the number of scales, as a representative of the near-centerline scales.

4. A composite scale

Since the problem involves events occurring at three dissimilar scales, other than the base scale y, a standard multiple scale method would formally require utilizing four scales, y, εy, $\varepsilon(1-y)^{-1}$, and $\varepsilon(1-y)^{-2}$, and integrating three times in order to reach a one-term expansion [2]. In light of the discussion presented in the previous paragraph, it can be argued that, in the case at hand, three representative scales, y, εy, and $\varepsilon(1-y)^{-3/2}$ may be used to attempt a uniformly valid expansion. Unfortunately, a multiple scale procedure using the aforementioned scales leads, in either situation, to dead ends. It is found that, for a closed form expression to be manageable here, the method of multiple scales will have to be limited to two variables, with one of them being the base scale y. Due to this restriction, a uniformly valid solution is tractable if a composite scale can be devised such as to provide the same geometric description that is available from the modified scales in their regions of applicability. To that end, the second step in our approach is to propose a composite scale, $y_1 = \varepsilon s(y)$, that is valid in the entire domain, and that reduces to the local characteristic scales. A nonunique scale function s is thus proposed

$$s(y) = \frac{y}{(1-y)^q} = \begin{cases} y & (y \to 0) \\ \frac{1}{(1-y)^{3/2}} & (y \to 1) \end{cases} \tag{4.1}$$

where the stretching exponent $q(y)$ is chosen to be a spatially sensitive function

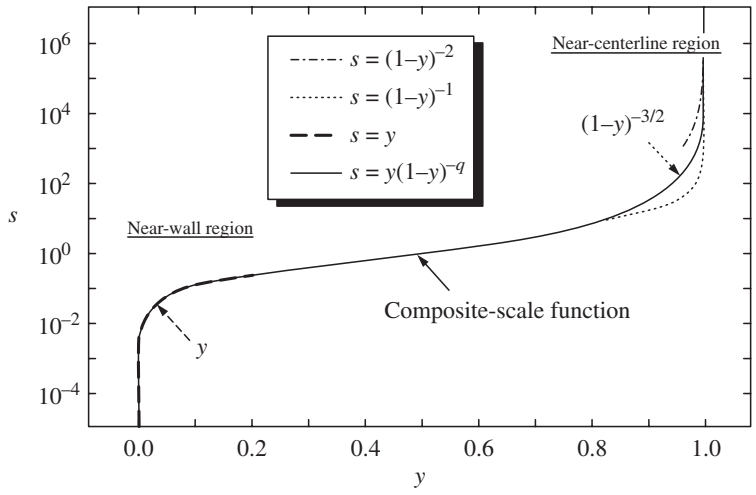

Figure 1.
Spatial distribution of the composite-scale function that matches efficaciously the widely dissimilar characteristic scales in their respective domains.

satisfying

$$q(y) = ay^b \rightarrow \begin{cases} 0 & (y \rightarrow 0) \\ 3/2 & (y \rightarrow 1) \end{cases} \tag{4.2}$$

The parameters a and b appearing in $q(y)$ can be determined to minimize the error between resulting analytical and numerical predictions which, in turn, is expected to provide smooth matching of the modified scales. In this problem, when $a = b = 3/2$, the resulting analytical predictions will match the numerical solution of (2.1) with an uncertainty that is smaller than the error associated with (2.1) itself, which is of order 10^{-3}. In Figure 1 above, the efficiency of the composite scale in matching the modified scales is illustrated graphically. In other problems, it could be speculated that a composite-scale function could be proposed, in general, as a candidate for matching the individual scales in their corresponding domains. The selection must be guided by a foreknowledge of the behavior of the proposed function. The geometric parameters in the proposed function could then be determined to minimize, for example, the maximum error in the resulting solution, or the error at a given point of interest.

5. A standard two-variable multiple scale expansion

Having identified and reduced the relevant scales to two, $y_0 = y$ and $y_1 = \varepsilon y/(1-y)^{q(y)}$, the third step in the current procedure is to invoke a standard multiple scale approach that consists of expanding the derivatives, as well as the

dependent variables in powers of the small parameter ε, in order to arrive at uniformly valid expansions. A generalized solution will be sought that is applicable to any characteristic scale $s(y)$. From the generalized expression, particular solutions corresponding to individual characteristic scales will be derived for comparison purposes.

5.1. A generalized two-variable expansion

The two scales to be used in the formal multiple scale expansion of (2.1) are: i) the base $y_0 \equiv y$, and ii) the modified scale $y_1 \equiv \varepsilon s(s) = \varepsilon s(y_0)$, written in the most general form to accommodate any scale function corresponding to a transformation of the transverse coordinate. As such, the value of the modified scale function may assume any of the following forms

$$s(y_0) = \begin{cases} y_0; & y \to 0 \\ (1-y_0)^{-q}; & y \to 1 \\ y_0(1-y_0)^{-q(y_0)}; & 0 \le y_0 \le 1 \end{cases} \tag{5.1}$$

Using the chain rule for differentiation, and carrying as many terms as is necessary to retain a final order of ε^2 the derivatives in (2.1) can be expanded as follows:

$$\frac{d}{dy} = \frac{\partial}{\partial y_0} + \varepsilon \frac{ds}{dy_0}\frac{\partial}{\partial y_1}; \quad \frac{d^2}{dy^2} = \frac{\partial^2}{\partial y_0^2} + O(\varepsilon) \tag{5.2}$$

After substitution of (5.2) into (2.1), the latter is transformed into a partial differential equation that is function of two coordinates y_0 and y_1. Using $\theta_0 = \pi y_0/2$ for brevity, (2.1) becomes

$$\varepsilon \frac{\partial^2 V_n}{\partial y_0^2} - \sigma U_y \frac{\partial V_n}{\partial y_0} - \varepsilon \sigma U_y \frac{ds}{dy_0}\frac{\partial V_n}{\partial y_1} + \left[i - \frac{\pi}{2}\sigma(1+\lambda_n)\sin\theta_0 \right] V_n + O(\varepsilon^2) = 0 \tag{5.3}$$

Following the multiple scale formal procedure, the dependent function is now written using a two-term expansion which is function of the two independent scales:

$$V_n(y_0, y_1) = V_n^{(0)}(y_0, y_1) + \varepsilon V_n^{(1)}(y_0, y_1) + O(\varepsilon^2) \tag{5.4}$$

Substituting the perturbed two-term expansion given by (5.4) into (5.3), rearranging and collecting terms of order ε^0 and ε^1, two first-order coupled partial differential equations must be satisfied for any value of ε. These are

$$-\sigma U_y \frac{\partial V_n^{(0)}}{\partial y_0} + \left[i - \frac{\pi}{2}\sigma(1+\lambda_n)\sin\theta_0 \right] V_n^{(0)} = 0 \tag{5.5}$$

$$-\sigma U_y \frac{\partial V_n^{(1)}}{\partial y_0} + \left[i - \frac{\pi}{2}\sigma(1+\lambda_n)\sin\theta_0 \right] V_n^{(1)} = \sigma U_y \frac{ds}{dy_0}\frac{\partial V_n^{(0)}}{\partial y_1} - \frac{\partial^2 V_n^{(0)}}{\partial y_0^2} \tag{5.6}$$

The boundary conditions given by (2.2) and (2.3) for V_n can be translated to the first perturbation term $V_n^{(0)}$ which must satisfy the same condition as V_n in the limit when $\varepsilon \to 0$, as can be clearly seen from (5.4). The resulting conditions that must be met by $V_n^{(0)}$ are

$$V_n^{(0)}(y_0 = 0) = 1 \tag{5.7}$$

$$\frac{\partial V_n^{(0)}}{\partial y_0}(y_0 = 1) = 0 \tag{5.8}$$

5.2. Nonsecular integration

The next step is to integrate (5.5), which is solely a function of the first scale, for the zeroth term $V_n^{(0)}$. The integration constant that can be a function of the second scale will have to be determined after substitution into (5.6) and examining the possibility of suppressing secular terms which, if retained, will cause the solution to become nonuniformly valid. Complete closure is later accomplished by applying the boundary conditions (5.7)-(5.8).

5.2.1. First integration. Equation (5.5) is a homogeneous first-order PDE with a variable coefficient that is solely a function of y_0. Direct integration yields

$$\begin{aligned} V_n^{(0)} &= C_1(y_1)\exp\left\{ (1+\lambda_n)\ln\cos\left(\frac{\pi}{2}y_0\right) + \frac{2i}{\pi\sigma}\ln\tan\left[\frac{\pi}{4}(1+y_0)\right] \right\} \\ &\equiv C_1(y_1)\chi(y_0) \end{aligned} \tag{5.9}$$

Since integration is carried out with respect to y_0 only, the constant of integration C_1 can, in general, be a function of y_1 as well.

5.2.2. Suppressing secular terms. First and second partial derivatives of $V_n^{(0)}$ are

$$\frac{\partial V_n^{(0)}}{\partial y_0} = C_1(y_1)\left[iSt\sec\theta_0 - \frac{\pi}{2}(1+\lambda_n)\tan\theta_0 \right]\chi(y_0) \tag{5.10}$$

$$\frac{\partial V_n^{(0)}}{\partial y_1} = \frac{dC_1(y_1)}{dy_1}\chi(y_0) \tag{5.11}$$

$$\begin{aligned} \frac{\partial^2 V_n^{(0)}}{\partial y_0^2} = \Big[&- St^2\sec^2\theta_0 + \frac{\pi^2}{4}(1+\lambda_n)(\lambda_n\tan^2\theta_0 - 1) \\ &- i\pi St\left(\frac{1}{2}+\lambda_n\right)\sec\theta_0\tan\theta_0 \Big] V_n^{(0)} \end{aligned} \tag{5.12}$$

Now by inserting (5.10)-(5.12) in (5.6), the right-hand-side becomes a source of secular terms. To remove secular terms which cause the solution to degenerate, a requirement that satisfies the symmetry condition, given by (5.8), is that the right-hand-side of (5.6) be zero

$$-\sigma U_y \frac{\partial V_n^{(1)}}{\partial y_0} + \Big[i - \frac{\pi}{2}\sigma(1+\lambda_n)\sin\theta_0 \Big] V_n^{(1)} = \Big\{ \sigma U_y \frac{ds}{dy_0}\frac{dC_1(y_1)}{dy_1} - C_1(y_1)\Big[-St^2\sec^2\theta_0 + \frac{\pi^2}{4}(1+\lambda_n)(\lambda_n\tan^2\theta_0 - 1) - i\pi St\left(\frac{1}{2}+\lambda_n\right)\sec\theta_0\tan\theta_0 \Big] \Big\} \chi(y_0) = 0 \tag{5.13}$$

yielding a first-order ODE that can be solved for C_1:

$$\frac{dC_1}{dy_1} - C_1 St \left[-St^2\sec^2\theta_0 + \frac{\pi^2}{4}(1+\lambda_n)(\lambda_n\tan^2\theta_0 - 1) - \pi St\left(\frac{1}{2}+\lambda_n\right)\sec\theta_0\tan\theta_0 \right] \sec\theta_0 \left(\frac{ds}{dy_0}\right)^{-1} = 0 \tag{5.14}$$

5.2.3. Second integration. Integration of (5.14), subject to satisfaction of the no-slip condition given by (5.7), allows the complete determination of C_1:

$$C_1(y) = \exp\Big\{ -\xi[\eta(y)\sec^3\theta - \eta(0)] + \xi\sigma^2\frac{\pi^2}{4}(1+\lambda_n)\big[\sec\theta\eta(y)(\lambda_n\tan^2\theta - 1) + \eta(0)\big] - i\pi\xi\sigma\left(\frac{1}{2}+\lambda_n\right)\eta(y)\sec^2\theta\tan\theta \Big\} \tag{5.15}$$

where the viscous parameter that controls the leading exponential term is

$$\xi = \frac{St^3}{Re_k} = \frac{\varepsilon}{\sigma^3} = \frac{v\omega^2 h}{V_b^3} \tag{5.16}$$

and the effective scale function $\eta(y)$, shown in Figure 2, controls the solution. This scale

$$\eta(y) \equiv s(y)\left(\frac{ds}{dy}\right)^{-1} \tag{5.17}$$

is found to be a smooth, positive, and skew-symmetric function.

5.2.4. General solution. Information from first and second perturbation levels can now be incorporated into the first term of the multiple scale expansion for V_n in (5.4). The result is

$$V_n = (\cos\theta)^{1+\lambda_n}\exp\Big\{ -\xi[\eta\sec^3\theta - \eta(0)] + \frac{\pi^2}{4}\xi\sigma^2(1+\lambda_n)\big[\eta\sec\theta(\lambda_n\tan^2\theta - 1) + \eta(0)\big] + \frac{2i}{\pi\sigma}\ln\tan\Big[\frac{\pi}{4}(1+y)\Big] - i\pi\xi\sigma\left(\frac{1}{2}+\lambda_n\right)\eta\sec^2\theta\tan\theta \Big\} \tag{5.18}$$

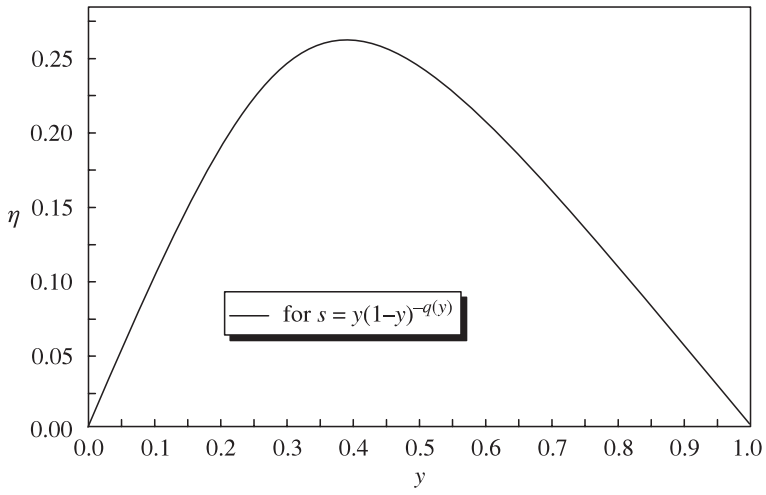

Figure 2.
Spatial distribution of the effective scale function $\eta(y)$ that controls the composite solution.

5.3. Particular solutions

In order to produce particular solutions in the various domains of interest, the only requirement will be a knowledge of the scale function and its derivative in order to determine the effective scale function $\eta(y)$ given by (5.17). The value of $\eta(0)$ will also be needed as necessitated by the velocity-adherence condition materialized in (5.18).

5.3.1. Near-wall solution. In this case, $s = y$, and $\eta = y$. Equation (5.18) becomes

$$V_n = (\cos\theta)^{1+\lambda_n} \exp\left\{-\xi y \sec^3\theta + \frac{\pi^2}{4}\xi\sigma^2(1+\lambda_n)[y\sec\theta(\lambda_n\tan^2\theta - 1)]\right. \quad (5.19)$$
$$\left. + \frac{2i}{\pi\sigma}\ln\tan\left[\frac{\pi}{4}(1+y)\right] - i\pi\xi\sigma\left(\frac{1}{2}+\lambda_n\right) y\sec^2\theta\tan\theta\right\}$$

5.3.2. Near-centerline solutions. Using $s = (1-y)^{-q}$, $\eta = (1-y)/q$, $q = 1, 2$, $r \equiv (1-y)$,

$$V_n = (\cos\theta)^{1+\lambda_n} \exp\left\{-\frac{\xi}{q}[r\sec^3\theta - 1] + \frac{\pi^2}{4q}\xi\sigma^2(1+\lambda_n)[r\sec\theta(\lambda_n\tan^2\theta - 1) + 1]\right. \quad (5.20)$$
$$\left. + \frac{2i}{\pi\sigma}\ln\tan\left[\frac{\pi}{4}(1+y)\right] - \frac{i\pi}{q}\xi\sigma\left(\frac{1}{2}+\lambda_n\right) r\sec^2\theta\tan\theta\right\}$$

5.3.3. Composite-scale solution. A uniformly valid solution is obtained when $s = yr^{-ay^b}$ resulting in

$$\frac{ds}{dy} = r^{-ay^b}(1 + ay^{b+1}r^{-1} - aby^b\ln r), \quad \eta = y[1 + ay^b(yr^{-1} - b\ln r)]^{-1} \quad (5.21)$$

$$V_n = (\cos\theta)^{1+\lambda_n} \exp\left\{-\xi\eta\sec^3\theta + \frac{\pi^2}{4}\xi\sigma^2(1+\lambda_n)\eta\sec\theta(\lambda_n\tan^2\theta - 1)\right. \quad (5.22)$$
$$\left. + \frac{2i}{\pi\sigma}\ln\tan\left[\frac{\pi}{4}(1+y)\right] - i\pi\xi\sigma\left(\frac{1}{2}+\lambda_n\right)\eta\sec^2\theta\tan\theta\right\}$$

6. Results and comparisons

For comparison purposes, a numerical solution to (2.1) is obtained using a classical fourth-order Runge-Kutta scheme, a shooting method, and superposition that takes advantage of the linearity in (2.1). The shooting procedure starts at the wall, and integrates the stiff differential equation back to the centerline using a step size of 10^{-6}. The maximum error associated with the numerical results is hence virtually insignificant.

Profiles of $V_n(y)$ corresponding to the composite-scale solution given by (5.22) are shown along with the numerical solution of (2.1) in Figure 3 and Figure 4 where real components are compared. In Figure 3, the results are compared at several typical values of the controlling parameters, and for the first value of λ_n. In Figure 4, the results are compared for the next four values of λ_n, and at a typical value of σ. The striking similarity between numerical and analytical results is reassuring and gets even better at smaller ε.

The function $V_n(y)$ is best described as an upward-traveling harmonic wave with an amplitude which suffers exponential damping with increasing distance from the wall. This damping is found to depend primarily on the viscous parameter, ξ; its dependence on σ is found to be insignificant as could be inferred from the spatial attenuation term of (5.22). In order to compare numerical and analytical results in a very wide range of physical parameters, and to provide further reassurance that the favorable trends depicted in Figures 3-4 are not merely fortuitous, the 99% based depth of penetration of V_n, a measure of the rotational region, is displayed in Figure 5, for the first two values of λ_n, as obtained from both numerical and multiple scale solutions. To that end, the depth of penetration is plotted, for a wide range of ε, versus the penetration number, $S_p \equiv \xi^{-1}$, which has been ascertained in this and similar studies ([4] and [5]) to be the agent in control of the spatial attenuation character of the rotational solution.

It should be pointed out that, despite the fact that (2.1) depends on both ε and σ, the perturbation analysis shows that the decay of rotational waves is controlled by a single nondimensional parameter, S_p, which groups both dynamic similarity parameters appearing in the governing differential equation. This important result could not have been foretold without the analytical derivation, since dimensional analysis and numerical solutions alone are not capable of revealing its existence. As it turns out, the larger the penetration number, the larger the penetration depth will be. Additionally, for small penetration numbers, the penetration depth varies linearly with the penetration number.

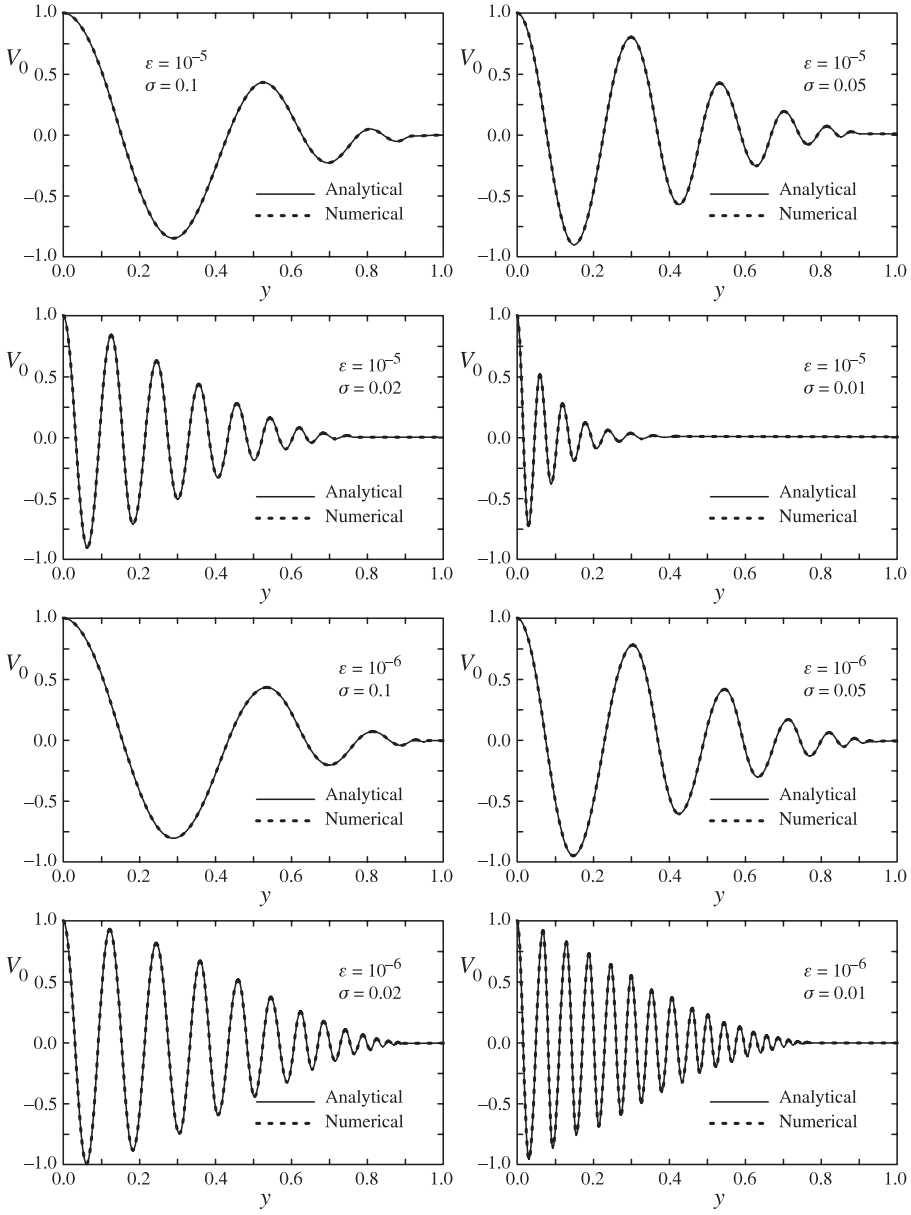

Figure 3.
Comparison of the composite-scale expansion for V_n to the numerical solution for several test cases corresponding to typical values of the control parameters and $n = 0$.

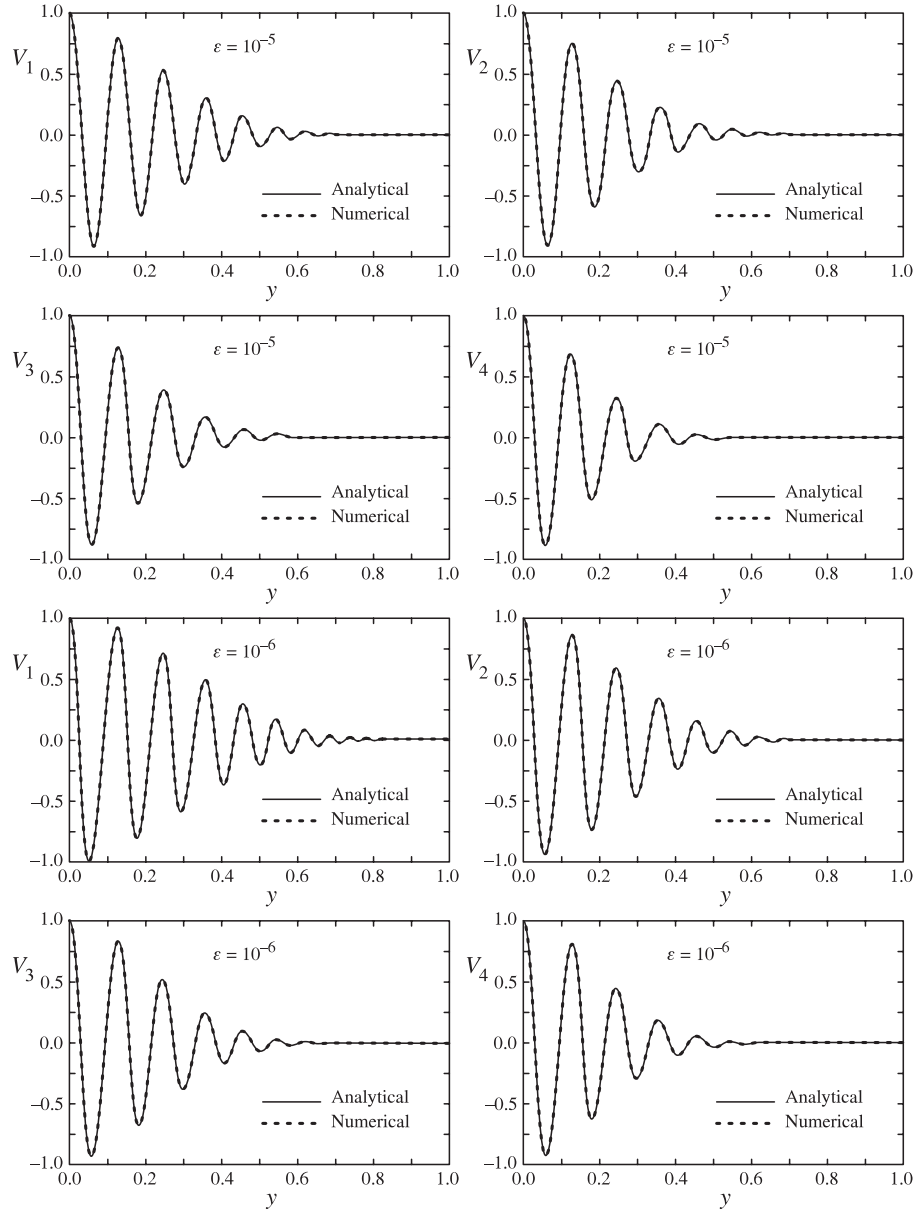

Figure 4.
Comparison of the composite-scale expansion for V_n to the numerical solution for several test cases corresponding to $n = 1, 2, 3, 4$, and $\sigma = 0.02$, corresponding to a typical value of the Strouhal number of 50.

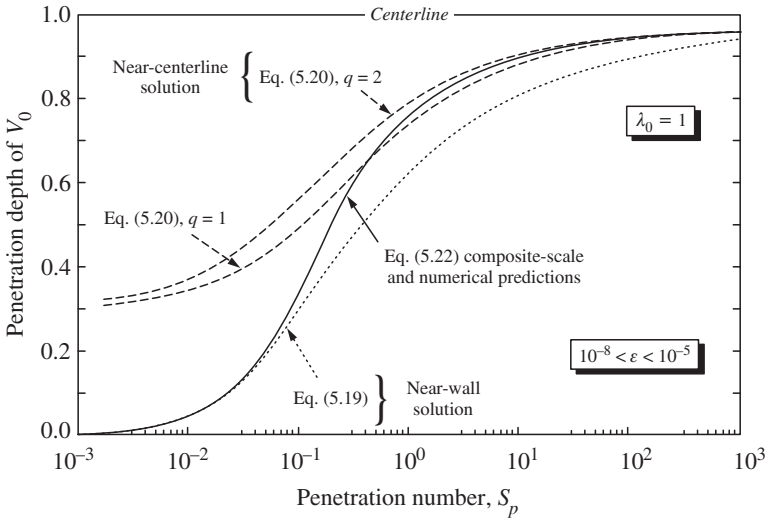

(a)

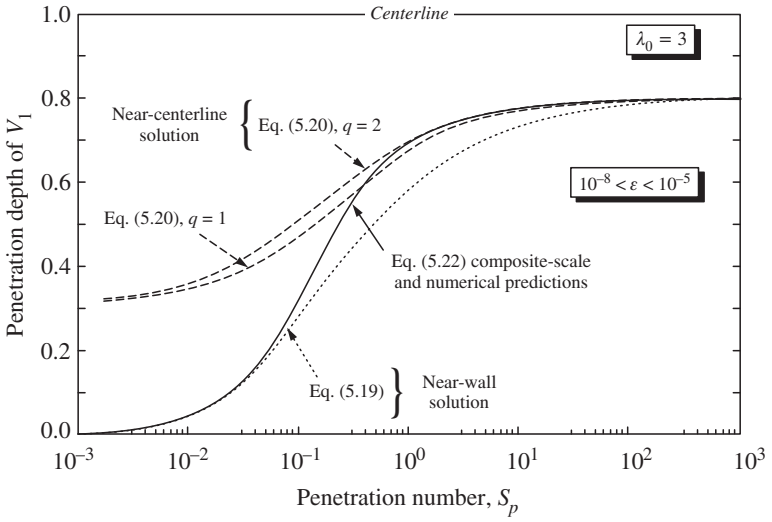

(b)

Figure 5.
Penetration depth of the velocity function V_n for a wide range of physical parameters showing an excellent agreement between multiple scale and numerical predictions for (a) $n = 0$, and (b) $n = 1$.

As one would expect in Figure 5, the multiple scale solution (5.19) that uses the near-wall scale and the numerical solution are in excellent agreement in the

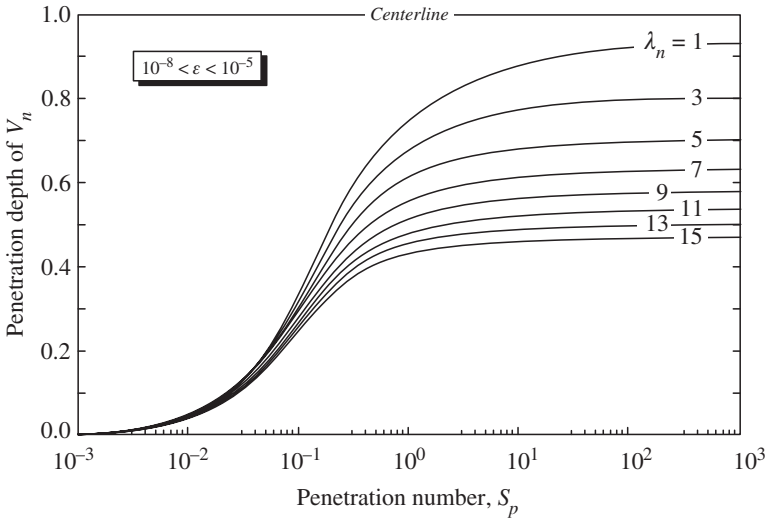

Figure 6.
Comparison of numerical and analytical predictions of the penetration depth of V_n for a wide range control parameters encompassing realistic physical settings and at several values of λ_n, $n = 0, 1, \ldots, 7$.

vicinity of the wall. Similarly, the centerline solutions (5.20) are in agreement with the numerical solution in their applicable domains, forming an envelope of undetermined size, as predicted by the scaling analysis of section 3. Note that the multiple scale solution (5.22) that uses the composite scale and the numerical solution concur in the entire domain and for a very wide range of physical parameters.

This close agreement between numerical and composite-scale predictions is further demonstrated in Figure 6 where the same trend is shown to persist at higher values of λ_n. Note that, for $\lambda_n > 15$ (not shown), the computational results begin to degenerate at high penetration numbers corresponding to invisicid or frictionless flows. The analytical results, however, remain unaffected.

Finally, it should be mentioned that, by contrast to traditional boundary layers, no single "inner" boundary-layer region could be located here, to which will correspond a unique "outer" region. This fact offers a plausible explanation for the reason behind the failure of matched asymptotic expansions. Furthermore, and contrary to conventional boundary layers, the depth of penetration diminishes with increasing viscosity.

7. Order Verification

In order to determine the order of the error associated with the composite-scale

expansion of V_n given by (5.22), and in order to show that the error tends to zero at the correct rate as $\varepsilon \to 0$, a simple yet powerful technique described by Bosley [1] will be invoked. Being ideally suited for both complicated and novel perturbation results, this technique is capable of verifying rigorously the quantitative accuracy of asymptotic expansions and ascertaining the order of accuracy, to ensure that no mistakes were made during the derivation process. Accordingly, if the error E_n associated with (5.22) could be represented by

$$E_n = K\varepsilon^{\alpha} \tag{7.1}$$

then α, representing the order of the error, could be approximated by the slope of the linear least-squares fit of the data generated by graphing $\log(E_n)$ versus $\log(\varepsilon)$ over a range of ε that is devoid of computational instabilities. In accordance with Bosley's technique, the calculated error E_n can be chosen, for the case at hand, to be the maximum absolute error over the domain of interest between analytical and accurate numerical results. For that purpose we define

$$E_n = \max_{\substack{y\in[0,1]\\ \sigma=const}} \left| V_{\text{numerical}}(y,n,\sigma,\varepsilon) - V_{\text{analytical}}(y,n,\sigma,\varepsilon) \right| \tag{7.2}$$

where the analytical component is calculated from (5.22) and the numerical component from solving (2.1) over the interval [0, 1] by use of a classical fourth-order Runge-Kutta scheme and a variable mesh size ranging from 10^{-6} to 10^{-9}. The maximum error defined by (7.2) is plotted versus ε, which is very finely spaced on the interval shown, in Figure 7, for a vast range of controlling parameters and $n = 0, 1$. Fitting linear least-squares to the data indicates that the order of the error approaches unity very rapidly as $\varepsilon \to 0$.

What is very interesting to note is that the regions where deviations from linearity are observed correspond to improbable or unrealistic physical settings, and to settings where the mathematical model used to approximate reality deteriorates. For instance, when $\sigma = 0.2$, the rate of decrease in the error starts fluctuating while maintaining the same overall asymptotic order. This can be attributed to the fact that $\sigma = 0.2$ corresponds to a quasi-steady field for which the mathematical model, intended for oscillatory fields, begins degenerating. Additionally, for large ε along lines of constant σ, the asymptotic rate of the error cannot be observed as clearly. This can be attributed to the fact that $\varepsilon = v\omega^{-1}h^{-2}$ cannot exceed certain limits by virtue of physical restrictions imposed on viscosity, frequency, and height of a channel.

A closer look at the asymptotic behavior of the error is given in Figure 8 for a typical value of σ, and a practical range of ε, for $n = 0, 1, 2$. The linear slopes obtained from least-squares are provided for two distinct ranges of ε with a high correlation coefficient of 1.0000. The results from least-squares are shown by thin solid lines, and the ranges corresponding to $\varepsilon \in [10^{-7}, 10^{-6}]$ and $\varepsilon \in [10^{-8}, 10^{-7}]$ are indicated by parentheses. Clearly, the slope approaches unity more rapidly at

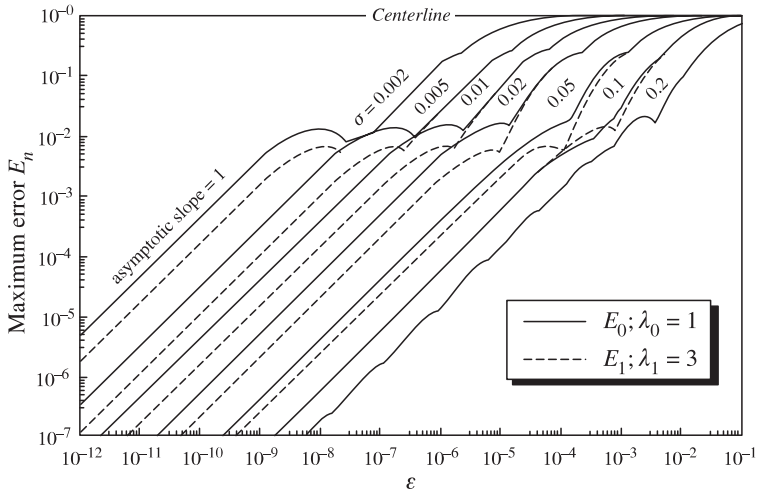

Figure 7.
Verification of the order of the error in the composite-scale expansion of V_n for a vast range of controlling parameters and the first two values of λ_n indicating a clear asymptotic behavior in wide ranges os ε.

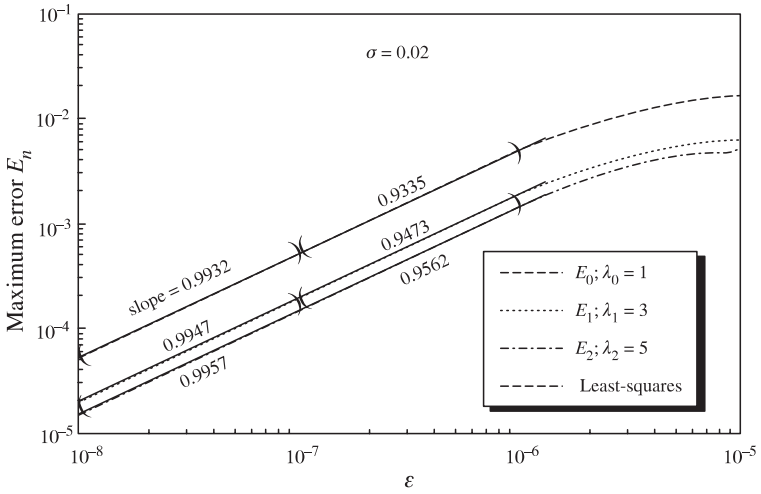

Figure 8.
Verification of the asymptotic order of the error for a practical range of parameters and $n = 0, 1, 2$, showing a consistent decrease in the error at a logarithmic rate that approaches unity as $\varepsilon \to 0$.

higher values of n and in ranges of smaller ε. This repetitive trend observed for other values of σ indicates that the error decreases consistently in ε according to

the correct asymptotic behavior; this behavior can be described by

$$E_n \underset{\varepsilon \to 0}{\longrightarrow} K\varepsilon \tag{7.3}$$

In conclusion, the error associated with the composite-scale technique presented here is established to be of $O(\varepsilon)$.

8. Closure

For a class of boundary-layer problems containing a small parameter and several dissimilar scales, a hybrid two-variable multiple scale procedure can be attempted. The method comprises three principal steps: 1) identification of the prevalent characteristic scales, 2) determination of a composite scale that matches the modified scales in their respective domains, and 3) application of a standard two-variable multiple scale expansion that includes the composite scale to arrive at accurate, uniformly valid solutions. The foregoing analysis furnishes guidelines to construct the composite scale which depends on the particular case at hand. It is hoped that more rigorous formalism can be established in the future to guide the selection of the composite scale function which might be derivable rather than established by trial, optimization, inspection or conjecture.

Since the main objective of the multiple scale approach is to seek approximate analytical expressions that would be uniformly valid, the scale-matching procedure presented here could be considered to be an honest and useful alternative, especially that other available methods ended in futility. Although not guaranteed to succeed under other circumstances, the method is likely to work in boundary-layer applications incorporating more than two characteristic scales. Such applications involving fast-changing processes will be dealt with in subsequent study and will be reported in our forthcoming work.

Acknowledgments

The author wishes to thank the editor and referees for very thorough corrections, suggestions and comments. In particular, thank you for the referral to Bosley's note which was instrumental in establishing the order of the error associated with the composite-scale technique.

References

[1] D. L. Bosley, A technique for the numerical verification of asymptotic expansions, *SIAM Rev.* **38** (1) (1996), 128–135.

[2] J. D. Cole and J. Aroesty, The blowhard problem-inviscid flows with surface injection, *Int. J. Heat Mass Transfer* **11** (1968), 1167–1183.

[3] J. Kevorkian and J. D. Cole, *Multiple Scale and Singular Perturbation Methods*, Springer-Verlag, New York 1996.
[4] J. Majdalani, Improved flowfield models in rocket motors and the Stokes layer with sidewall injection, Ph. D. dissertation, University of Utah (1995).
[5] J. Majdalani and W. K. Van Moorhem, A multiple-scales solution to the acoustic boundary layer in solid rocket motors, *J. Propulsion Power (JPP)* **13** (2) (1997), 186–193.
[6] J. Murdock, *Perturbations: Theory and Methods*, Wiley, New York 1991.
[7] J. Murdock, Validity of the multiple scale method for very long intervals, *J. Appl. Math. Phys. (ZAMP)* **47** (1996), 760–789.
[8] D. C. Wilcox, *Perturbation Methods in the Computer Age*, DCW Industries, Inc., La Cañada, CA 1995.

Joseph Majdalani
Department of Mechanical and Industrial Engineering
Marquette University
Milwaukee WI 53233, USA
(e-mail: maji@marquette.edu)

(Received: June 17, 1997; revised: October 21, 1997)